Redundant and unique roles of retinol dehydrogenases in the mouse retina

Akiko Maeda*, Tadao Maeda*, Wenyu Sun*, Houbin Zhang†, Wolfgang Baehr†‡§, and Krzysztof Palczewski*¶

*Department of Pharmacology, Case Western Reserve University, Cleveland, OH 44106-4965; and Departments of †Ophthalmology and Visual Sciences, ‡Biology, and §Neurobiology and Anatomy, University of Utah, Salt Lake City, UT 84132

Edited by Thaddeus P. Dryja, Novartis Institutes for Biomedical Research, Inc., Boston, MA, and approved October 15, 2007 (received for review August 8, 2007)

Highly abundant short-chain alcohol dehydrogenases (RDHs) in the retina were assumed to be involved in the recycling of 11-*cis*-retinal chromophore in the visual cycle. Mutations in human RDH genes are associated with *Fundus albipunctatus*, a mild form of night blindness (*RDH5*) and an autosomal recessive, childhood-onset severe retinal dystrophy (*RDH12*). *Rdh12* knockout mice were found to be susceptible to light-induced photoreceptor apoptosis, whereas *Rdh5* and *Rdh8* knockout mice displayed only delayed dark adaptation. However, each knockout mouse eventually regenerated normal levels of visual pigments, suggesting that RDHs compensate for each other in the visual cycle. Here, we established RDH double knockout (*Rdh8*$^{-/-}$*Rdh12*$^{-/-}$) and triple knockout (*Rdh5*$^{-/-}$*Rdh8*$^{-/-}$*Rdh12*$^{-/-}$) mice generated on various genetic backgrounds including a rod α-transducin knockout to test cone function. RDH activity was severely reduced in *Rdh8*$^{-/-}$Rdh12$^{-/-}$ retina extracts, whereas *Rdh8*$^{-/-}$ RDH activity was intermediate and *Rdh12*$^{-/-}$ RDH activity was reduced only slightly. Surprisingly, all multiple knockout mice produced sufficient amounts of the chromophore to regenerate rhodopsin and cone pigments *in vivo*. Three-month-old *Rdh8*$^{-/-}$*Rdh12*$^{-/-}$ mice characteristically displayed a slowly progressing rod–cone dystrophy accompanied by accumulation of *N*-retinylidene-*N*-retinylethanolamine (A2E), a toxic substance known to contribute to retinal degeneration. A2E accumulation and retinal degeneration were prevented by application of retinylamine, a potent retinoid cycle inhibitor. The results suggest that RDH8 and RDH12 are dispensable in support of the visual cycle but appear to be key components in clearance of free all-*trans*-retinal, thereby preventing A2E accumulation and photoreceptor cell death.

cone | photoreceptors | rhodopsin | rod

Regeneration of 11-*cis*-retinal, the chromophore of visual pigments in photoreceptor cells, is essential for vision (1). Photoactivation of rhodopsin and cone pigments causes isomerization of 11-*cis*-retinal to all-*trans*-retinal, which is released from the pigment and recycled in a pathway termed the visual (retinoid) cycle (2). Two reactions in this cycle are catalyzed by retinol dehydrogenases (RDHs). Based on biochemical approaches, several RDHs of the visual cycle have been identified. Reduction of all-*trans*-retinal to all-*trans*-retinol in photoreceptors is catalyzed by all-*trans*-RDHs (RDH8 and RDH12) (3, 4), whereas oxidation of 11-*cis*-retinol to 11-*cis*-retinal in the retinal pigment epithelium (RPE) is catalyzed by 11-*cis*-RDHs (RDH5 and RDH11) (5). RDH10 and retinal short-chain dehydrogenase reductase 1 (retSDR1) expressed in the RPE and photoreceptor cells, respectively, also have been reported to display all-*trans*-RDH activity (6, 7).

Deletion of photoreceptor RDH8 in mice causes only a mild phenotype consisting of delayed dark adaptation (8). RDH12, a member of a novel subfamily of four retinol dehydrogenases (RDH11–14), exhibits activity toward all-*trans*- and *cis*-retinals (4) and other aldehydes (9). In humans, RDH12 mutations have been reported to be associated with a severe, early-onset autosomal recessive retinal dystrophy called Leber congenital amaurosis (LCA) (10), characterized by progressive rod–cone dystrophy and severe macular atrophy (11). The phenotype of RDH12 knockout mice is milder than that of humans carrying RDH12-null alleles, and the retinal pathology does not resemble LCA exactly (12, 13). However, we have observed that RDH12-deficient mice show a greater susceptibility to light-induced photoreceptor apoptosis, suggesting that retinal degeneration may correlate with light exposure (12).

Here, we established knockout lines of mice (*Rdh8*$^{-/-}$ and *Rdh12*$^{-/-}$ on WT and rod α-transducin knockout backgrounds and *Rdh8*$^{-/-}$*Rdh12*$^{-/-}$ and *Rdh5*$^{-/-}$*Rdh8*$^{-/-}$*Rdh12*$^{-/-}$ on a WT background) to explore the roles of these three RDH isozymes in the visual cycle of rod and cone photoreceptors. First, our data showed that the majority of all-*trans*-RDH activity in mouse retina extracts was attributable to RDH8 and RDH12. Second, *Rdh8*$^{-/-}$*Rdh12*$^{-/-}$ mice revealed retarded all-*trans*-retinal clearance, over-accumulation of *N*-retinylidene-*N*-retinylethanolamine (A2E), and slowly progressive retinal degeneration. Third, triple RDH knockout mice still produced enough 11-*cis*-retinal to regenerate rhodopsin and cone pigments. These findings suggest that A2E buildup is in part responsible for the retinal degeneration observed in RDH knockout animal models. Moreover, these results provide direct evidence that other RDH activities are sufficient to support visual cycle in mice.

Results

RDH Activity in RDH Knockout Mouse Retinas. *Rdh8*$^{-/-}$ and *Rdh12*$^{-/-}$ knockout mice with a pigmented background were backcrossed to generate *Rdh8*$^{-/-}$*Rdh12*$^{-/-}$ double knockouts. The double knockouts were fertile and showed no obvious developmental abnormalities. By using an *in vitro* analysis, we measured the effect of disrupting the all-*trans*-RDH genes on reduction of all-*trans*-retinal. All-*trans*-retinal was applied exogenously to dissected retinas, and all-*trans*-RDH activity was determined by the rate of all-*trans*-retinol production. Interestingly, all-*trans*-RDH activity was nearly absent ($\approx$2% of WT) in the *Rdh8*$^{-/-}$*Rdh12*$^{-/-}$ retinas (Fig. 1 *A* and *B*). Furthermore, after 5 min of incubation, RDH8 activity accounted for $\approx$70% of the total all-*trans*-RDH activity in the retina, whereas RDH12 was responsible for $\approx$30% of this activity (Fig. 1*B*). Thus, both RDH8 and RDH12 isozymes exhibited all-*trans*-RDH activity in the retina, but RDH8 was the main contributor to the total RDH activity. Although, RDHs are typically unregulated enzymes, it cannot be excluded that during retinal extract preparation, a

Author contributions: A.M., T.M., and K.P. designed research; A.M., T.M., W.S., H.Z., and W.B. performed research; A.M., W.S., H.Z., and W.B. contributed new reagents/analytic tools; A.M., T.M., W.S., H.Z., W.B., and K.P. analyzed data; and A.M., T.M., W.B., and K.P. wrote the paper.

The authors declare no conflict of interest.

This article is a PNAS Direct Submission.

¶To whom correspondence should be addressed at: Department of Pharmacology, School of Medicine, Case Western Reserve University, 10900 Euclid Avenue, Cleveland, OH 44106-4965. E-mail: kxp65@case.edu.

This article contains supporting information online at www.pnas.org/cgi/content/full/0707477104/DC1.

© 2007 by The National Academy of Sciences of the USA

NEUROSCIENCE

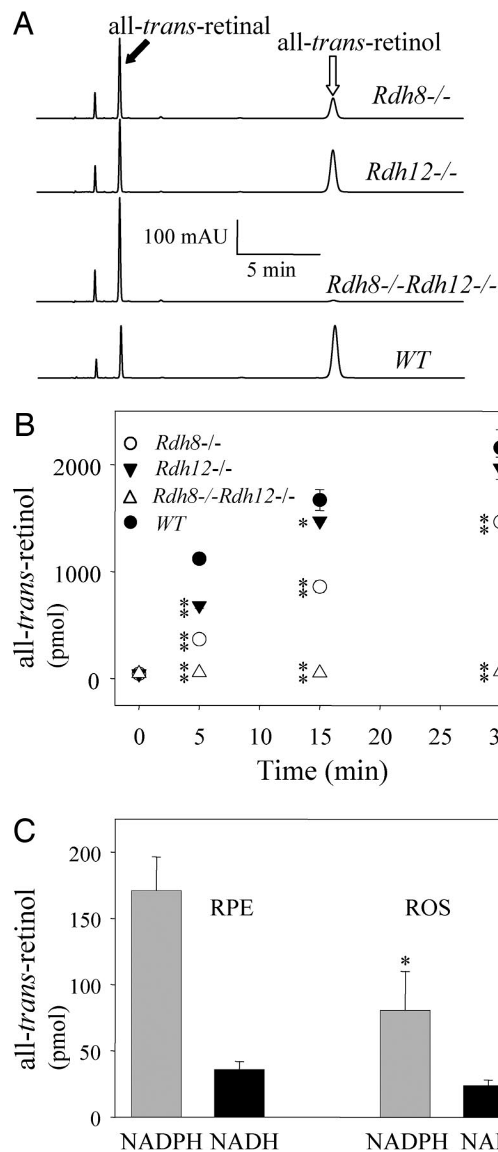

Fig. 1. RDH activity in the retina, ROS, and RPE of $Rdh8^{-/-}$, $Rdh12^{-/-}$, and $Rdh8^{-/-}Rdh12^{-/-}$ mice at 6 weeks of age. (*A*) All-*trans*-RDH activities of half of a mouse retina (homogenates with the reaction buffer) were determined by monitoring the reduction of all-*trans*-retinal to all-*trans*-retinol. A representative HPLC chromatogram after 5 min of incubation is shown ($n > 5$). mAU, milli-absorbance units. (*B*) Time course of the all-*trans*-retinol production (reduction of all-*trans*-retinal) in mouse retina. Bars indicate SEM ($n > 5$). *, $P < 0.01$; **, $P < 0.0001$. (*C*) All-*trans*-RDH activities of the ROS (60 μg) and the RPE (60 μg) from $Rdh8^{-/-}Rdh12^{-/-}$ mice were analyzed. Bars indicate SEM ($n > 2$). *, $P < 0.01$.

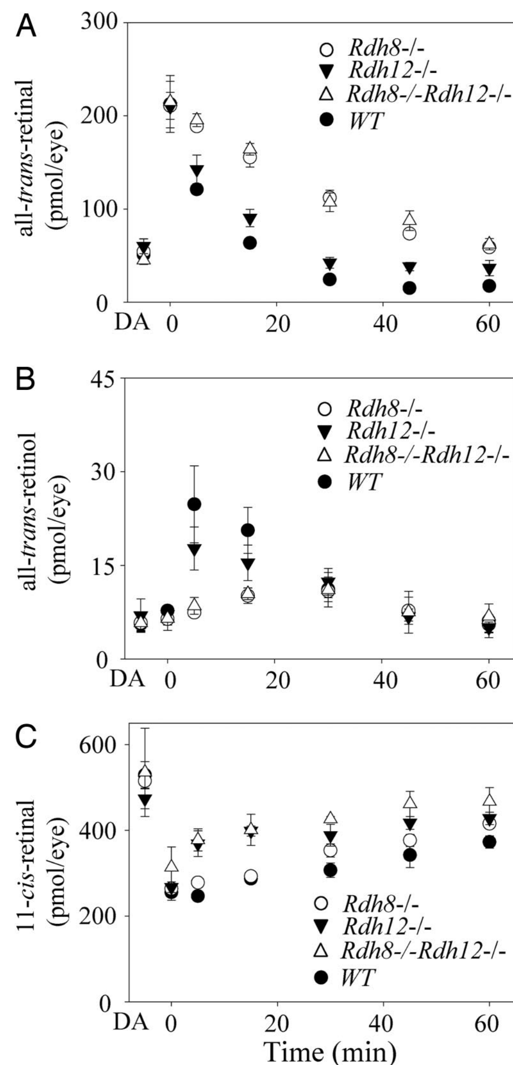

Fig. 2. Kinetics of all-*trans*-retinal reduction and 11-*cis*-retinal formation in $Rdh8^{-/-}$, $Rdh12^{-/-}$, and $Rdh8^{-/-}Rdh12^{-/-}$ mice at 6 weeks of age. Retinoids were quantified by HPLC in samples collected at different time points after a flash that bleached ≈35% of the visual pigment. (*A*) Changes in all-*trans*-retinal levels as a function of time after flash. (*B*) Changes in all-*trans*-retinol levels. (*C*) Changes in 11-*cis*-retinal levels. Mice were reared under 12-h dark/12-h light conditions. Bars indicate SEM ($n > 3$).

hypothetical RDH lost an unidentified cofactor that was essential for its activity.

To examine whether the RPE plays a role in all-*trans*-retinal clearance, we tested RDH activity of RPE prepared from $Rdh8^{-/-}Rdh12^{-/-}$ mice and found it to exhibit NAD(H)-dependent *cis*-RDH activity as predicted (data not shown) (14). All-*trans*-RDH activity in the RPE purified from $Rdh8^{-/-}Rdh12^{-/-}$ mice was 2-fold higher than observed in the rod outer segments (ROS) from these mice (Fig. 1*C*). These data suggest that the RPE can augment the clearance of all-*trans*-retinal in mouse retina and that additional enzymes possibly participate in the retinal all-*trans*-RDH pathway.

To determine whether RDH5, as a major RDH in the RPE, might have all-*trans*-RDH activity *in vivo*, we established RDH triple knockout mice ($Rdh5^{-/-}Rdh8^{-/-}$ $Rdh12^{-/-}$). In the dark, the level of all-*trans*-retinal was 5 ± 1 pmol per eye and, after ≈80% rhodopsin bleach, increased to 412 ± 11 pmol per eye. Clearance of all-*trans*-retinal in triple knockout mice was 18% slower than that in $Rdh8^{-/-}Rdh12^{-/-}$ mice at 45 min of dark adaptation, consistent with only minor *in vivo* all-*trans*-RDH activity of RDH5 in the RPE. However, all-*trans*-retinal was still reduced to all-*trans*-retinol *in vivo* in the absence of RDH5, RDH8, and RDH12, and the visual cycle operated efficiently to regenerate rhodopsin [supporting information (SI) Fig. 6].

Flow of Retinoids in $Rdh8^{-/-}Rdh12^{-/-}$ Mice. To explore the contributions of RDH8 and/or RDH12 to retinoid flow, we analyzed retinoid levels at various times after an intense flash that bleached ≈35% of the rhodopsin in pigmented RDH knockout mice. As expected for 6-week-old pigmented animals (Met-450–RPE65), bleaching caused formation of all-*trans*-retinal (Fig. 2*A*), which was reduced to all-*trans*-retinol (Fig.

Fig. 3. Full-field ERG responses of RDH mutant mice with different genetic backgrounds. (*A*) ERG responses were recorded from $Rdh8^{-/-}Rdh12^{-/-}$ and WT mice at 3 months of age under scotopic and photopic conditions. The *a*- and *b*-wave amplitudes are plotted as a function of light intensity. Both *a*- and *b*-wave amplitudes were significantly attenuated in $Rdh8^{-/-}Rdh12^{-/-}$ mice as compared with WT mice. *, $P < 0.01$; **, $P < 0.0001$. (*B*) Recovery of *a*-wave amplitudes after constant light stimulation. Dark-adapted mice were exposed to intense illumination (500 cd·m^{-2}) for 3 min, and the recovery of *a*-wave amplitudes was monitored with single-flash ERG (−0.2 log cd·s·m^{-2}) every 5 min for 60 min. The recovery rate was significantly attenuated in $Rdh8^{-/-}$, $Rdh12^{-/-}$, and $Rdh8^{-/-}Rdh12^{-/-}$ mice (**, $P < 0.0001$) compared with WT mice (n = 5 each). (*C*) The *a*- and *b*-wave response amplitudes from $Gnat1^{-/-}Rdh8^{-/-}$, $Gnat1^{-/-}Rdh12^{-/-}$, and $Gnat1^{-/-}$ mice are plotted vs. light intensity. There was no significant difference in cone responses between mutant mice.

2*B*). The retinal reduction kinetics were slower in $Rdh8^{-/-}$, $Rdh12^{-/-}$, and $Rdh8^{-/-}Rdh12^{-/-}$ mouse retinas as compared with WT retinas. $Rdh8^{-/-}$ and $Rdh8^{-/-}Rdh12^{-/-}$ mice showed more impaired kinetics than $Rdh12^{-/-}$ mice, indicating that RDH8 plays a predominant role for all-*trans*-retinal clearance in the retina (Fig. 2*B*). Whereas the *in vitro* all-*trans*-RDH assay showed a 98% suppression in retinas from $Rdh8^{-/-}Rdh12^{-/-}$ mice (Fig. 1 *A* and *B*), *in vivo* retinoid analyses revealed only delayed reduction kinetics, implying that the living retina compensated for loss of RDH8 and RDH12 in the retinoid cycle. Although the kinetics of 11-*cis*-retinal formation was accelerated in mice lacking RDH12 and differed between various RDH knockouts (Fig. 2*C*), the chromophore was regenerated to prebleached levels (data not shown).

Impaired Visual Function and Dark Adaptation in $Rdh8^{-/-}Rdh12^{-/-}$ Mice. To test for visual function, we used electroretinography (ERG) to examine 3-month-old pigmented $Rdh8^{-/-}Rdh12^{-/-}$ mice maintained in a 12-h light/12-h dark cycle. Amplitudes of scotopic and photopic *a*- and *b*-waves were significantly reduced in $Rdh8^{-/-}Rdh12^{-/-}$ mice (Fig. 3*A*), suggesting retinal degeneration. Amplitudes of flicker ERGs from $Rdh8^{-/-}Rdh12^{-/-}$ mice also were also reduced compared with those from WT mice (data not shown). In contrast to both scotopic and photopic *a*- and *b*-waves, which were unchanged in 6-week-old $Rdh8^{-/-}Rdh12^{-/-}$ mice (data not shown), single RDH8 and RDH12 knockout mice at age of 6 weeks and 3 months did not display this phenotype.

To assess the rate of dark adaptation, we exposed 6-week-old mice to intense Ganzfeld background light at 500 cd·m^{-2} for 3 min (≈70% rhodopsin bleach) and then returned them to the dark. Recovery of the ERG responses (dark adaptation), measured by monitoring amplitudes of *a*-waves after exposure to the constant illumination, was significantly slower in $Rdh8^{-/-}Rdh12^{-/-}$ mice than in WT mice ($P < 0.0001$, Fig. 3*B*). We concluded that in mice at 6 weeks of age, ERG responses were nearly normal but that dark adaptation after strong bleach was delayed, despite of accelerated 11-*cis*-retina formation. This delay may be explained by the lingering presence of the opsin/all-*trans*-retinal complex, which desensitizes photoreceptor cells (15).

RDH8 and RDH12 could play a more critical role in the visual cycle in cone photoreceptors. Because rod and cone ERG responses overlap, rod responses must be eliminated to monitor pure cone responses (16). Thus, we backcrossed $Rdh8^{-/-}$ and $Rdh12^{-/-}$ single knockouts with rod α-transducin [photoreceptor G protein (GNAT1)] knockout mice that lack rod signaling to test the function of cone photoreceptors. At 6 weeks of age, ERG analyses of $Gnat1^{-/-}Rdh8^{-/-}$ and $Gnat1^{-/-}Rdh12^{-/-}$ mice were found to be similar to those from control $Gnat1^{-/-}$ mice (Fig. 3*C*), suggesting that cone photoreceptors function normally. In contrast, the impairment of chromophore production in $Gnat1^{-/-}Rpe65^{-/-}$ mice resulted in highly attenuated ERG cone responses (17) (unpublished data).

Changes in Rhodopsin Levels and Retinal Structure in $Rdh8^{-/-}Rdh12^{-/-}$ Double Knockout Mice. In order to assess the loss of retinal outer segments in relation to phenotype, we examined the levels of 11-*cis*-retinal that correlate to the levels of rhodopsin formed in the retina. Pigmented $Rdh8^{-/-}Rdh12^{-/-}$ mice with Met-450–RPE65 and albino $Rdh8^{-/-}Rdh12^{-/-}$ mice with Leu-450–RPE65 had similar amounts of 11-*cis*-retinal at 6 weeks of age (pigmented, 531.5 ± 26.5 pmol per eye; albino, 527.6 ± 12.3 pmol per eye) (Fig. 4*A*). But at 3 months of age, animals maintained in a 12-h light/12-h dark cycle showed lesser amounts of 11-*cis*-retinal (pigmented, 434.9 ± 24.3 pmol per eye; albino, 408.4 ± 37.0 pmol per eye) compared with dark-maintained animals (Fig. 4*A*). Even further reduction of the levels of 11-*cis*-retinal was detected in 6-month-old albino $Rdh8^{-/-}Rdh12^{-/-}$ mice (367.0 ± 27.0 pmol per eye) whereas dark-maintained animals had similar amounts of 11-*cis*-retinal (pigmented, 580.6 ± 54.7 pmol per eye; albino, 516.5 ± 21.1 pmol per eye) as 6-week-old animals (Fig. 4*A*). Amounts of 11-*cis*-retinal were unchanged in 6-month-old WT mice maintained in the 12-h light/12-h dark cycle (pigmented, 527.7 ± 23.3 pmol per eye; albino, 505.8 ± 16.4 pmol per eye) compared with 6-week-old mice maintained in the 12-h light/12-h dark cycle. These 11-*cis*-retinal quantification results correlated well with the histological changes noted in $Rdh8^{-/-}Rdh12^{-/-}$ mice.

Light microscopy of retinas from pigmented $Rdh8^{-/-}Rdh12^{-/-}$ double knockout mice at 3 months of age under 12-h dark/12-h ≈10 lux light conditions revealed ≈20% shortening in the length of the ROS compared with WT mice over the entire retina (Fig. 4 *B*–*I*). In contrast, no apparent abnormalities were found in the retinas of $Rdh8^{-/-}Rdh12^{-/-}$ mice raised under 12-h dark/12-h light conditions at 6 weeks of age or in retinas of 3-month-old $Rdh8^{-/-}Rdh12^{-/-}$ mice raised in the dark (data not shown). The most affected area of the ROS was the central part of the inferior retina. Obvious changes in cone photoreceptor cells were not detected, but irregular arrangements of cone photoreceptor cells were sometimes seen in pigmented $Rdh8^{-/-}Rdh12^{-/-}$ mice with Leu-450–RPE65 at 3 months of age or older (Fig. 4 *F* and *G*). Numbers of cone photoreceptor cells were decreased in Met-450–RPE65 mice older than 8 months of age (Fig. 4 *H* and *I*). No retinal changes were observed in single knockouts of *Rdh8* or *Rdh12* mice of the same age (data not shown). Light exposure was required to induce retinal degeneration when the *RDH12* gene was disrupted, as shown previously (8, 12).

NEUROSCIENCE

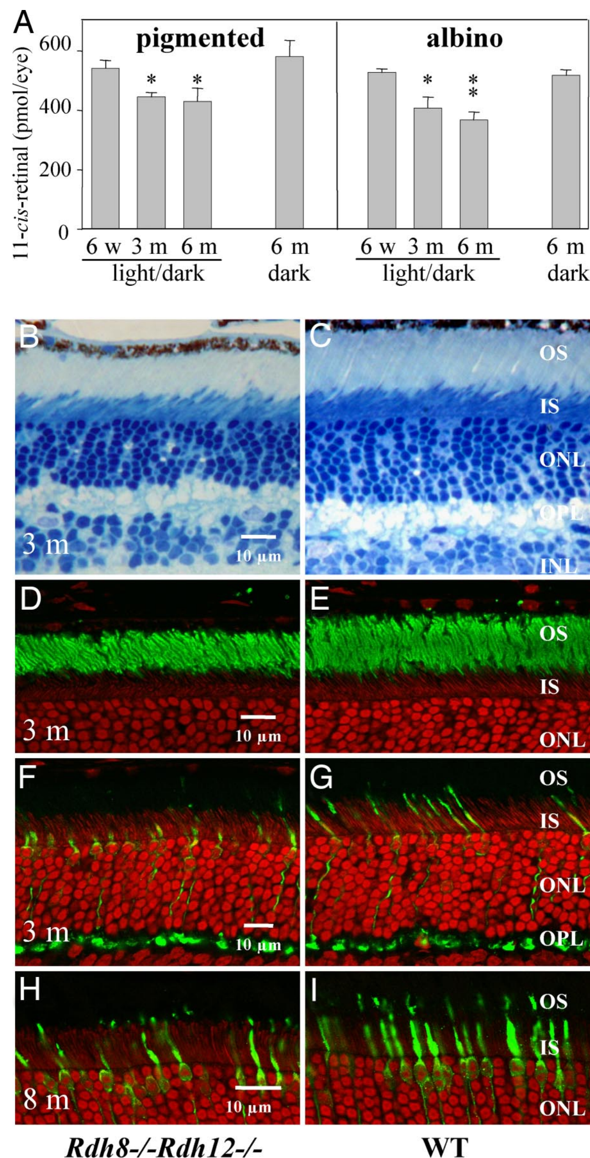

Fig. 4. 11-*cis*-Retinal content in the eye and morphological changes in the retina of RDH mutant mice with different genetic backgrounds raised under different light conditions. (*A*) Amounts of 11-*cis*-retinal in retinas of 6-week-old, 3-month-old, and 6-month-old mice maintained in a 12-h light/12-h dark cycle and 6-month-old mice maintained in the dark. Pigmented *Rdh8*$^{-/-}$*Rdh12*$^{-/-}$ with Met-450–RPE65 and albino *Rdh8*$^{-/-}$*Rdh12*$^{-/-}$ with Leu-450–RPE65 were analyzed. Error bars indicate SEM ($n > 3$). *, $P < 0.01$; **, $P < 0.0001$. (*B* and *C*) Micrographs of the inferior retina from the left eye of 3-month-old pigmented (Leu-450–RPE65) *Rdh8*$^{-/-}$*Rdh12*$^{-/-}$ and WT mice. (*D* and *E*) Immunocytochemistry of the inferior retina from the right eye of the same mice as Fig. 1 *B* and *C*. Green, anti-rhodopsin staining. (*F* and *G*) Immunocytochemistry of the inferior retina from 3-month-old pigmented *Rdh8*$^{-/-}$*Rdh12*$^{-/-}$ mice. Green, anti-cone arrestin. (*H* and *I*) Immunocytochemistry of the inferior retina from 8-month-old pigmented *Rdh8*$^{-/-}$*Rdh12*$^{-/-}$ mice. Green, anti-cone arrestin. OS, outer segment; IS, inner segment; ONL, outer nuclear layer; OPL, outer plexiform layer.

Accumulation of A2E in the Eyes of RDH Knockout Mice. A2E, the major hydrophobic and cytotoxic component of lipofuscin, is formed from two molecules of all-*trans*-retinal and one molecule of ethanolamine (Fig. 5*A*). Reduced activity in RDH8 and RDH12 knockouts generates an excess of all-*trans*-retinal (Fig. 2*A*), predicting increased levels of A2E that are toxic for the retina. Thus, we used HPLC to quantify A2E levels in retinas

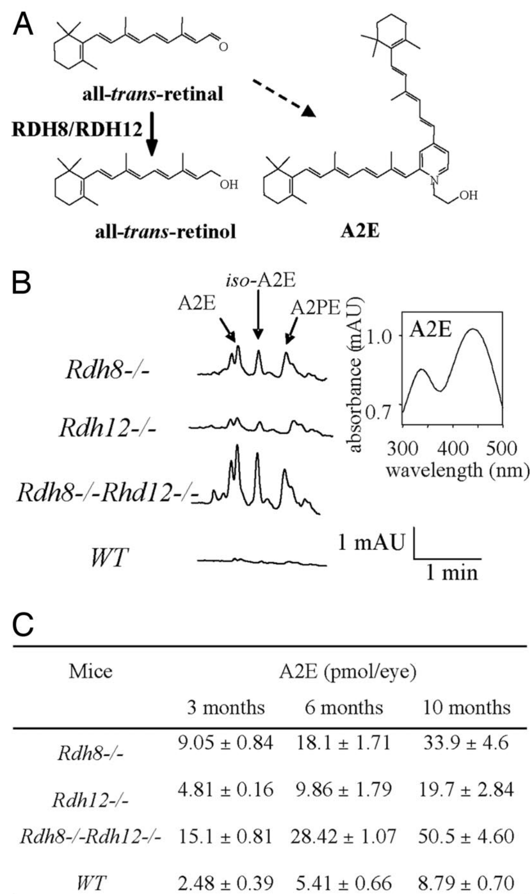

Mice	A2E (pmol/eye)		
	3 months	6 months	10 months
Rdh8-/-	9.05 ± 0.84	18.1 ± 1.71	33.9 ± 4.6
Rdh12-/-	4.81 ± 0.16	9.86 ± 1.79	19.7 ± 2.84
Rdh8-/-Rdh12-/-	15.1 ± 0.81	28.42 ± 1.07	50.5 ± 4.60
WT	2.48 ± 0.39	5.41 ± 0.66	8.79 ± 0.70

Fig. 5. Formation and buildup of A2E in double knockout retina. (*A*) Reduction of all-*trans*-retinal in the photoreceptor catalyzed by RDH8 and RDH12. A2E, an aberrant side product, is produced by the condensation of two molecules of all-*trans*-retinal molecules with phosphatidylethanolamine. A2E accumulates in the RPE as a result of the phagocytosis of outer segments of RPE. *Iso*-A2E is a *trans*-isomer of A2E at carbon 13–14. (*B*) (*Left*) Representative HPLC chromatogram of A2E, *iso*-A2E, and A2PE (intermediate of A2E formation) detected in *Rdh8*$^{-/-}$, *Rdh12*$^{-/-}$, and *Rdh8*$^{-/-}$*Rdh12*$^{-/-}$ and WT mice at the age of 3 months. (*Right*) UV/visible spectrum of A2E from the *Rdh8*$^{-/-}$ mouse. (*C*) Levels of A2E in the retina/RPE of *Rdh8*$^{-/-}$, *Rdh12*$^{-/-}$, *Rdh8*$^{-/-}$*Rdh12*$^{-/-}$, and WT mice. A2E [±SE ($n > 3$)] was measured in mice at 3, 6, and 10 months of age.

from *Rdh8*$^{-/-}$, *Rdh12*$^{-/-}$, and *Rdh8*$^{-/-}$*Rdh12*$^{-/-}$ mice at different ages. At 3 months of age (Fig. 5*B*), elevated A2E levels were detected in all mutant animals. The levels steadily increased over a period of 10 months (Fig. 5*C*). In the *Rdh8*$^{-/-}$*Rdh12*$^{-/-}$ mice, A2E levels at 10 months were ≈5.7-fold higher than in age-matched WT mice. By comparison, our *Abca4*$^{-/-}$ mice (unpublished data) at age of 3 months had ≈10-fold higher than in age-matched WT mice.

Retinylamine Protects Against the Accumulation of A2E in the *Rdh8*$^{-/-}$*Rdh12*$^{-/-}$ Retina. Because accumulation of A2E is caused by a higher flow of intermediates through the retinoid cycle, we tested the retinoid cycle inhibitor retinylamine (Ret-NH_2) to protect against retinal degeneration (18). *Rdh8*$^{-/-}$*Rdh12*$^{-/-}$ pigmented mice were treated with Ret-NH_2 for 2 months and maintained in a 12-h light/12-h (<50 lux) dark cycle. At 3 months of age, Ret-NH_2 treatment had successfully maintained retinal structure (SI Fig. 7 *A* and *B*). The thickness of the outer nuclear layer plotted in SI Fig. 7*B* also shows that Ret-NH_2 prevented photoreceptor cell degeneration. Amounts of 11-*cis*-retinal,

measured by HPLC, were 531.6 ± 57.6 pmol per eye for Ret-NH_2-treated mice vs. 371.2 ± 48.7 pmol per eye for vehicle-treated mice (SI Fig. 7*C*). Ret-NH_2-treated mice had 0.45 ± 0.4 pmol per eye of A2E, whereas vehicle-treated mice showed 17.4 pmol per eye (SI Fig. 7*D*). Thus, our results suggest that retinal degeneration observed in *Rdh8*$^{-/-}$*Rdh12*$^{-/-}$ mice is caused in part by light exposure, leading to A2E accumulation.

Discussion

Photoreceptor outer segments, where RDH8 resides (3), contain most of the visual-function-related proteins, whereas the inner segments, where RDH12 is located, are responsible for photoreceptor cell metabolism (12, 13). The RPE, which provides metabolic support for the retina, contains *cis*-specific RDH5 (19). *In vivo*, loss of RDH8 activity in *Rdh8*$^{-/-}$ mice was manifested by only a mildly delayed clearance of all-*trans*-retinal released from photoactivated pigments, whereas loss of RDH12 activity in *Rdh12*$^{-/-}$ mice did not produce an obviously abnormal phenotype (Fig. 2) (12, 13). Herein, we report effects of deletions of RDHs in *Rdh8*$^{-/-}$*Rdh12*$^{-/-}$ double knockout and *Rdh5*$^{-/-}$*Rdh8*$^{-/-}$*Rdh12*$^{-/-}$ triple knockout mice on the production of 11-*cis*-retinal in the retina of mice. Surprisingly, dark-adapted double and triple RDH knockout mice adequately regenerated their visual pigments, thereby providing evidence that other RDH enzyme(s) complement these deleted enzymes in the mouse visual cycle. Mice with ablation of both RDH8 and RDH12 exhibited only mild, light-dependent retinal degeneration with delayed dark adaptation, reduced clearance of all-*trans*-retinal after bleach, and concurrent accelerated 11-*cis*-retinal production. As a result of all-*trans*-retinal buildup in the retina, faster rhodopsin regeneration, and because of a higher flux of retinoid through the visual cycle, elevated levels of A2E were observed in these RDH knockout mice.

Our *in vitro* assays indicated that RDH8 and RDH12 together accounted for >98% of the all-*trans*-RDH activity in rodent retina. Moreover, our experiments revealed that RDH8 accounted for most of the all-*trans*-RDH activity in the eye (70% RDH8 vs. 30% RDH12 assayed *in vitro*; Fig. 1 *A* and *B*). Together, these results suggest not only that RDH8 is one of the major all-*trans*-RDHs in mice but also that it plays a more dominant role than RDH12 in the mouse retinoid cycle. Because both RDH8 and RDH12 are responsible for all-*trans*-retinal reduction in photoreceptors, extensive retinoid analyses were undertaken to assess retinoid flow. Surprisingly *in vivo*, even *Rdh5*$^{-/-}$*Rdh8*$^{-/-}$*Rdh12*$^{-/-}$ mice regenerated 11-*cis*-retinal with rates quite comparable with WT mice. When retinal degeneration was not evident in 6-week-old *Rdh8*$^{-/-}$*Rdh12*$^{-/-}$ mice, retinoid flow was similar, as found in *Rdh8*$^{-/-}$ and *Rdh12*$^{-/-}$ single knockout mice of the same age (Fig. 2), suggesting that RDH8 and RDH12 do not substitute for each other in mouse retinoid metabolism. These results change our current understanding of reactions in the visual cycle that were unpredictable from previous reports. It appears that in mice, several RDHs may compensate for each other *in vivo*, so multiple knockouts may be required to discern the individual effects of the *cis*- and *trans*-RDHs. This analytic approach is complicated by the lack of strict substrate specificity among these enzymes. The large number of additional RDHs from both short- and medium-chain alcohol dehydrogenase families and other dehydrogenases may prevent further genetically driven analysis of individual RDH function at this time.

Surprisingly, only mild retinal degeneration was observed in *Rdh8*$^{-/-}$*Rdh12*$^{-/-}$ mice reared under 12-h dark/12-h (≈10 lux) light conditions, whereas no structural changes were seen in single knockout *Rdh8*$^{-/-}$ or *Rdh12*$^{-/-}$ mice of the same age. Because the changes in the flow of retinoids through the visual cycle alone could not account for this phenotype, we sought alternative explanations for the light-triggered retinal degeneration found in *Rdh8*$^{-/-}$*Rdh12*$^{-/-}$ mice. Consequently, we explored the possibility of increased A2E accumulation as a cause of retinal degeneration. A2E is toxic to retinal cells, and all-*trans*-retinal clearance is tightly connected to A2E formation. Indeed, we found that *Rdh12*$^{-/-}$ mice had a lower level of A2E than *Rdh8*$^{-/-}$ mice, which displayed more delayed all-*trans*-RDH kinetics. Also, the amounts of A2E noted in *Rdh8*$^{-/-}$*Rdh12*$^{-/-}$ mice were the highest of all animals that we studied (Fig. 5). This effect of A2E can be exacerbated by accelerated 11-*cis*-retinal regeneration in *Rdh12*$^{-/-}$ mice of differing genetic backgrounds (Fig. 2*C*) (12), leading to light-induced photoreceptor apoptosis. Thus, high A2E levels could contribute significantly to the retinal light-induced damage found in our *Rdh8*$^{-/-}$*Rdh12*$^{-/-}$ mice. This argument is strengthened by reversal of A2E accumulation and retinal degeneration when the inhibitor of the visual cycle Ret-NH_2 was used over a period.

These RDH mouse models are reminiscent of a mouse model of the Stargardt disease, *Abca4*$^{-/-}$ mice, which also exhibit delayed dark adaptation, evidence of photoreceptor degeneration, accumulation of A2E, and its precursors in the RPE (20). ATP-binding cassette transporter (ABCR), which is coded by the *Abca4* gene, is a ATP-dependent transporter of all-*trans*-retinal of its derivatives from the internal membranous structures of photoreceptors, the disk membranes. This clearance of all-*trans*-retinal from intradiscal space or from the cytosol of the photoreceptor cells is key for their cellular functional survival and consistent with the phenotype of *Abca4*$^{-/-}$ and *Rdh8*$^{-/-}$*Rdh12*$^{-/-}$ mice.

Materials and Methods

Animals. All animal procedures and experiments were approved by the Case Western Reserve University Animal Care Committees and the Institutional Animal Care and Use Committee of the University of Utah and conformed to both the recommendations of the American Veterinary Medical Association Panel on Euthanasia and the Association of Research for Vision and Ophthalmology. Mice were maintained under complete darkness or in a 12-h light/12-h dark cycle. All manipulations were done under dim red light transmitted through a No. 1 safelight filter (transmittance >560 nm; Kodak).

Rdh8$^{-/-}$ and *Rdh12*$^{-/-}$ mice were generated and genotyped as described previously (8, 12). These pigmented mice were maintained on a C57BL/6 background with a methionine residue at position 450 (Met-450) and 129Sv/Ev with a leucine residue (Leu-450) in the RPE65 polypeptide. *Rdh8*$^{-/-}$ or *Rdh12*$^{-/-}$ albino mice (Leu-450–RPE65) were generated by cross-breeding single knockout *Rdh8*$^{-/-}$ or *Rdh12*$^{-/-}$ pigmented mice to BALB/c mice with Leu-450–RPE65 for more than five generations. Pigmented and albino *Rdh8*$^{-/-}$*Rdh12*$^{-/-}$ mice were generated by cross-breeding *Rdh8*$^{-/-}$ and *Rdh12*$^{-/-}$ mice. *Rdh5*$^{-/-}$ (21) and *Gnat1*$^{-/-}$ (16) mice were generated and genotyped as described previously. C57BL/6 (Met-450–RPE65), BALB/c (Leu-450–RPE65), and 129Sv/Ev (Leu-450–RPE65) mice were purchased from Taconic and The Jackson Laboratory.

ERG. Full-field ERG recordings, flicker ERGs, and single-flash recordings after intense constant illumination were performed by previously published methods (8).

Histology and Immunocytochemistry. Histological and immunocytochemical procedures have been described previously (22). Cone cells were stained anti-cone arrestin antibody (a generous gift of Cheryl Craft, University of Southern California, Los Angeles, CA). Anti-rhodopsin antibody B6–30 used in this study has been characterized previously (23).

NEUROSCIENCE

Retinoid and A2E Analyses. All experimental procedures related to extraction, derivatization, and separation of retinoids from dissected mouse eyes were carried out as described previously (8).

Preparation of Mouse ROS and RPE. Preparation of osmotically intact ROS and RPE from 40 mouse eyes was performed as described previously (24, 25).

RDH Assays. All-*trans*-RDH activity was assessed by monitoring the production of all-*trans*-retinol (reduction of all-*trans*-retinal), and *cis*-RDH activity was examined as reported previously (24). The reduction reaction mixture (100 μl) contained *n*-dodecyl-β-maltoside (1 mM) with NAD(P)H (1 mM) in 10 mM phosphate buffer (pH 7.0), and the reaction was initiated by the addition of all-*trans*-retinal (final concentration, 20 μM). Half of a retina or the ROS was used for each all-*trans*-RDH assay, and the RPE was used for the *cis*-RDH assay. Reaction mixtures were incubated at 37°C for various periods and terminated with 300 μl of methanol, and retinoids were extracted twice with 300 μl of hexane and analyzed by HPLC by using 10% ethyl acetate in hexane.

We thank Drs. C. Driessen and J. Janssen (University of Nijmegen, Nijmegen, The Netherlands) for RDH5 mice, Dr. J. Lem (Tufts University, Boston, MA) for *Gnat1*$^{-/-}$ mice, and Dr. L. Webster (Case Western Reserve University) for comments on the manuscript. This work was supported by National Institutes of Health Grants EY09339, P30 EY11373, and EY08123 and the Foundation Fighting Blindness. H.Z. and W.B. also were supported in part by the Knights Templar Eye Foundation.

1. Palczewski K (2006) *Annu Rev Biochem* 75:743–767.
2. Travis GH, Golczak M, Moise AR, Palczewski K (2007) *Annu Rev Pharmacol Toxicol* 47:469–512.
3. Rattner A, Smallwood PM, Nathans J (2000) *J Biol Chem* 275:11034–11043.
4. Haeseleer F, Jang GF, Imanishi Y, Driessen CA, Matsumura M, Nelson PS, Palczewski K (2002) *J Biol Chem* 277:45537–45546.
5. Kim TS, Maeda A, Maeda T, Heinlein C, Kedishvili N, Palczewski K, Nelson PS (2005) *J Biol Chem* 280:8694–8704.
6. Haeseleer F, Huang J, Lebioda L, Saari JC, Palczewski K (1998) *J Biol Chem* 273:21790–21799.
7. Wu BX, Chen Y, Fan J, Rohrer B, Crouch RK, Ma JX (2002) *Invest Ophthalmol Vis Sci* 43:3365–3372.
8. Maeda A, Maeda T, Imanishi Y, Kuksa V, Alekseev A, Bronson JD, Zhang H, Zhu L, Sun W, Saperstein DA, *et al.* (2005) *J Biol Chem* 280:18822–18832.
9. Kasus-Jacobi A, Ou J, Bashmakov YK, Shelton JM, Richardson JA, Goldstein JL, Brown MS (2003) *J Biol Chem* 278:32380–32389.
10. Janecke AR, Thompson DA, Utermann G, Becker C, Hubner CA, Schmid E, McHenry CL, Nair AR, Ruschendorf F, Heckenlively J, *et al.* (2004) *Nat Genet* 36:850–854.
11. Perrault I, Hanein S, Gerber S, Barbet F, Ducroq D, Dollfus H, Hamel C, Dufier JL, Munnich A, Kaplan J, *et al.* (2004) *Am J Hum Genet* 75:639–646.
12. Maeda A, Maeda T, Imanishi Y, Sun W, Jastrzebska B, Hatala DA, Winkens HJ, Hofmann KP, Janssen JJ, Baehr W, *et al.* (2006) *J Biol Chem* 281:37697–37704.
13. Kurth I, Thompson DA, Ruther K, Feathers KL, Chrispell JD, Schroth J, McHenry CL, Schweizer M, Skosyrski S, Gal A, *et al.* (2007) *Mol Cell Biol* 27:1370–1379.
14. Jang GF, McBee JK, Alekseev AM, Haeseleer F, Palczewski K (2000) *J Biol Chem* 275:28128–28138.
15. Jager S, Palczewski K, Hofmann KP (1996) *Biochemistry* 35:2901–2908.
16. Calvert PD, Krasnoperova NV, Lyubarsky AL, Isayama T, Nicolo M, Kosaras B, Wong G, Gannon KS, Margolskee RF, Sidman RL, *et al.* (2000) *Proc Natl Acad Sci USA* 97:13913–13918.
17. Bemelmans AP, Kostic C, Crippa SV, Hauswirth WW, Lem J, Munier FL, Seeliger MW, Wenzel A, Arsenijevic Y (2006) *PLoS Med* 3:e347.
18. Golczak M, Kuksa V, Maeda T, Moise AR, Palczewski K (2005) *Proc Natl Acad Sci USA* 102:8162–8167.
19. Simon A, Hellman U, Wernstedt C, Eriksson U (1995) *J Biol Chem* 270:1107–1112.
20. Mata NL, Tzekov RT, Liu X, Weng J, Birch DG, Travis GH (2001) *Invest Ophthalmol Vis Sci* 42:1685–1690.
21. Driessen CA, Winkens HJ, Hoffmann K, Kuhlmann LD, Janssen BP, Van Vugt AH, Van Hooser JP, Wieringa BE, Deutman AF, Palczewski K, *et al.* (2000) *Mol Cell Biol* 20:4275–4287.
22. Baehr W, Karan S, Maeda T, Luo DG, Li S, Bronson JD, Watt CB, Yau KW, Frederick JM, Palczewski K (2007) *J Biol Chem* 282:8837–8847.
23. Adamus G, Zam ZS, Arendt A, Palczewski K, McDowell JH, Hargrave PA (1991) *Vision Res* 31:17–31.
24. Jang GF, Van Hooser JP, Kuksa V, McBee JK, He YG, Janssen JJ, Driessen CA, Palczewski K (2001) *J Biol Chem* 276:32456–32465.
25. Liang Y, Fotiadis D, Filipek S, Saperstein DA, Palczewski K, Engel A (2003) *J Biol Chem* 278:21655–21662.